RSC Advances

PAPER

View Article Online
View Journal | View Issue

Check for updates

Cite this: RSC Adv., 2017, 7, 39803

Dynamic/quasi-static stab-resistance and mechanical properties of soft body armour composites constructed from Kevlar fabrics and shear thickening fluids†

Jianbin Qin, Guangcheng Zhang,* Lisheng Zhou, Jiantong Li and Xuetao Shi*

Soft body armour composites were constructed by combining Kevlar fabrics with different quantities of shear thickening fluid (STF). In particular, the quantity of the added STF and the mechanical properties of these composites were systemically explored. The dynamic and quasi-static knife-stabbing resistance and the quasi-static mechanical properties of these composites were both significantly enhanced in comparison to those of neat Kevlar fabric. The composites were much lighter, thinner and more flexible than the neat Kevlar fabric and, with an optimal quantity of added STF, could not even be penetrated. However, the dynamic knife-stabbing resistance of the fabric became poor when the amount of added STF was higher than 100 wt%. The tensile strength of the composites could be increased from 40% to 80% and the tearing strength could be increased by nearly eight times that of the neat Kevlar fabric by increasing the concentration of added STF. Yarn pull-out testing suggested that the triggered shear thickening contributed to the increase of the friction between yarns or filaments, resulting in improvements in the dynamic and quasi-static properties of these composites. Moreover, these composites are suitable for use as soft body armour materials due to their good adaptability to high and low speeds conditions.

Received 9th July 2017
Accepted 4th August 2017

DOI: 10.1039/c7ra07549a

rsc.li/rsc-advances

Open Access Article. Published on 15 August 2017. Downloaded on 15/01/2018 07:53:55.
This article is licensed under a Creative Commons Attribution 3.0 Unported Licence.

1. Introduction

Shear-thickening fluid (STF) is a novel suspension whose viscosity can increase with increasing shear rate or applied stress. Under a high-speed shear rate, the viscosity of the STF increases dramatically, and it appears as a solid-like material. Moreover, the STF immediately reverses its state to a liquid-like material when the impact stress is removed.[1–5] In other words, STFs are self-adjusting smart materials.

Hoffman has proposed that shear thickening in concentrated suspensions results from the order–disorder transition.[6,7] Other researchers have demonstrated that the shear-thickening behavior in concentrated colloidal suspensions is caused by hydrodynamic lubrication forces between particles, resulting in the formation of a non-equilibrium, self-organized microstructure that develops under strong flows, denoted as hydroclusters.[8–12] Recently, jamming and dilation for shear thickening in dense dispersions have been described.[13–17] The idea is that the particle system in suspension dilates, *i.e.*, particles tend to expand when they are made to flow.

Shear thickening behavior is not desirable in some industries, such as food, paint and ceramics, where it leads to issues such as failure of mixer motors due to overloading and mixer blade damage in industrial situations.[1,18] However, STFs have attracted much attention, and they have been used in the design of protective smart composites over the past few decades.[19–30]

Decker *et al.* performed systematic research on the stab resistance of STF-treated fabrics for the first time in 2006.[22] They concluded that the stab resistances of STF-treated Kevlar and nylon fabrics were improved significantly over those of the neat fabric targets; dramatic improvements in puncture resistance were observed, while slight increases in knife protection were also observed. Decker *et al.* also proposed that the added STF reduced the mobility of filaments and yarns, which led to the improvements in stab resistance. The added weight percentage of STF was between 20 and 30 for all STF-treated fabrics in this study.[22] Li *et al.* demonstrated that the dynamic stab resistance of UHMWPE fabric was significantly enhanced by the presence of an STF. They proposed that the impregnating STF accelerated the transverse response of the UHMWPE fabric and increased the inter-yarn friction. The role of the STF in the STF-treated fabrics was important; however, the quantity of the impregnated STF in the fabrics was ignored in this study.[24] Selim and Melih found that multi-phase STFs resulted in further improvements in the stab resistance of STF-treated fabrics with

Key Laboratory of Space Applied Physics and Chemistry, Ministry of Education, School of Natural and Applied Sciences, Northwestern Polytechnical University, Xi'an 710072, China. E-mail: zhangguc@nwpu.edu.cn; shixuetao@nwpu.edu.cn

† Electronic supplementary information (ESI) available. See DOI: 10.1039/c7ra07549a

Open Access Article. Published on 15 August 2017. Downloaded on 15/01/2018 07:53:55.
This article is licensed under a Creative Commons Attribution 3.0 Unported Licence.

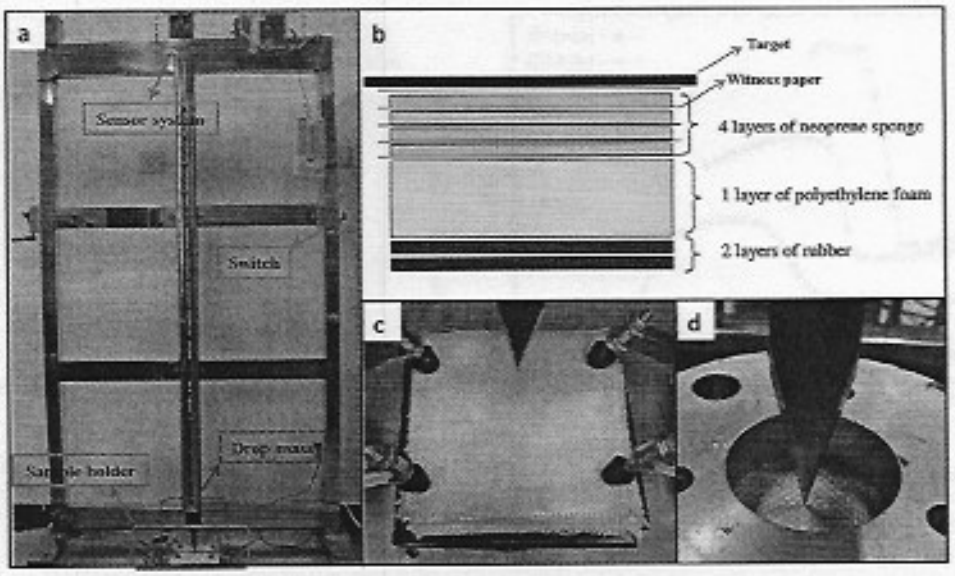


Fig. 1 (a) Measuring installation, (b) installation of target and (c) target holder for the dynamic knife-stabbing tests, and (d) sample holder for the quasi-static knife-stabbing tests.

installation, as shown in Fig. 1a. Fig. 1b and c show the installation of the target and the target holder. The drop mass contained a cylinder steel and the knife; the total mass was about 4500 g. The air drag on the drop mass was ignored, and the impacting energy was calculated by eqn (2). The conditions of the dynamic knife-stabbing tests are shown in Table 1.

$$\text{Impacting energy} = m \times g \times h \quad (2)$$

where m is the mass of the drop; g is the gravitational acceleration, 9.8 m s^{-2}; and h is the vertical distance between the tip of the knife blade and the impacting point.

The quasi-static knife-stabbing tests were performed with the electronic universal testing machine; the sample was clamped by a self-designed cylindrical holder, as shown in Fig. 1d. Sufficient force was introduced to clamp the specimen with the bolts in order to avoid slippage. The instrument measured the generated force, and the absorbed energy was simultaneously calculated for the sample against the displacement.

The quasi-static mechanical properties, tensile strength and tearing strength in warp direction, were measured with the electronic universal testing machine, referencing ASTM D5034 and ASTM D2261, respectively. The single yarn pull-out tests were performed as follows: the bottom portion of single yarn at the center of each specimen was intentionally cut so that it could be pulled out without elastic deformation or failure. The top of that yarn was loaded into the upper clamp of the testing machine, while the lower edge of the rectangular fabric specimen was mounted in a clamped holding fixture, as shown in the inset of Fig. 10a. Referencing ASTM D2256, the tensile strength of the single yarn was tested with the electronic universal testing machine. The flexural rigidities of the samples were measured with electronic rigidity equipment (LLY-01B) as stated in option A (cantilever test) of ASTM D1388.

Table 1 Impact conditions for dynamic knife-stabbing tests

Drop mass (kg)	Drop height (cm)	Theoretical impact velocity (m s^{-1})	Theoretical impact energy (J)
4.50	10	1.96	4.41
	15	2.94	6.62
	20	3.92	8.82
	25	4.90	11.03
	30	5.88	13.23

3. Results and discussion

3.1 Properties of STFs

As shown in Fig. 2, STFs with different concentrations exhibit shear thickening behavior. With increasing concentration of STF, corresponding to the onset increase of viscosity, the critical shear rate decreases. For the STF with 70 wt% silica microspheres, the viscosity increases by nearly two orders of magnitude in the shear thickening region, and it presents jamming at high shear rates. The 70 wt% STF displayed such prominent shear thickening properties that it was selected to be combined with Kevlar fabrics. Moreover, the STF showed complete reversibility and instantaneous response (as shown in Fig. S1 and S2 in the ESI†). This indicates that the STF can be used repeatedly and responds quickly to external conditions.

3.2 Dynamic and quasi-static knife-stabbing resistance

As shown in Table 2 and Fig. 3, the targets of neat and PEG-treated Kevlar fabrics are composed of twelve layers, while the targets of STF-prepared composites are constructed of nine

Open Access Article. Published on 15 August 2017. Downloaded on 15/01/2018 07:53:55.
This article is licensed under a Creative Commons Attribution 3.0 Unported Licence.

force to ascend oscillatorily, as shown in Fig. 5c–f. This implies that the friction between yarns or filaments increases significantly with the introduction of STF, and the mobility of yarns or filaments in the composites is much weaker than that of the neat or PEG-treated Kevlar fabrics. The immobile yarns resist knife puncture until they are cut off one by one in the composites, and the cutting-off force of the yarn is much higher than the force that causes it to slip; therefore, the generated force is very high and oscillatory, and the absorbed energy increases evidently. With increasing quantity of added STF, the friction between yarns may increase, causing the resistance and the absorbed energy to increase. The friction between yarns declines upon the introduction of PEG-400, which lubricates the yarns in the Kevlar fabrics; therefore, the generated force and absorbed energy decrease. In other words, it is the STF that causes the increases in the generated force and the absorbed energy.

3.3 Quasi-static mechanical properties of STF-prepared Kevlar fabric composites

In the quasi-static tensile tests, compared with the neat Kevlar fabric, as the load increased steeply, the tensile strength increased significantly and the elongation at break decreased for the STF-prepared Kevlar fabric composites, as shown in Fig. 6a. Apparently, the yarns are crimped in the neat Kevlar fabrics and the STF-prepared composites at the initial state and are progressively straightened along the loading direction.[33] The straightened length is similar for the same size samples of the neat Kevlar fabric and the composites. Therefore, the displacement, corresponding to the loading peak in the composites, is the same as that in the neat Kevlar fabric. The friction between yarns in the composites is higher than that in the neat Kevlar fabric, leading to an increase in the straightened resistance. Most yarns in the composites were broken after the loading peak was reached (as shown in Fig. S4b in the ESI†), and

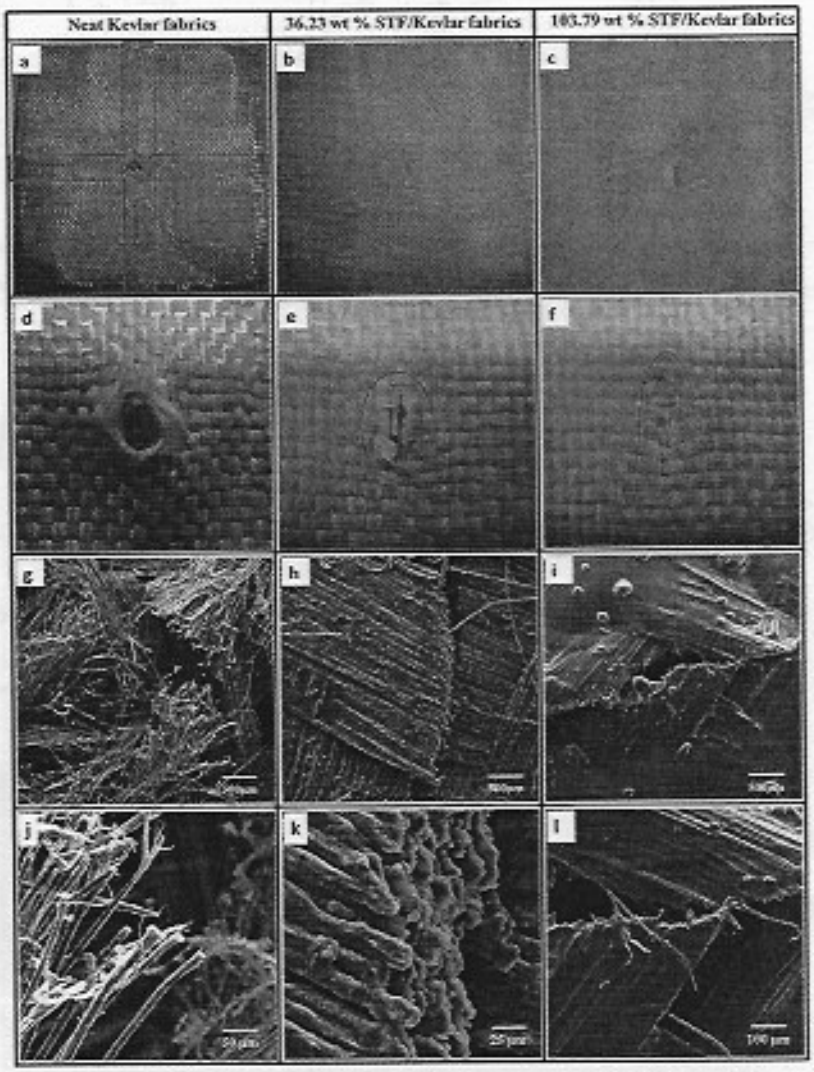


Fig. 4 Photographs and SEM images of broken samples from the dynamic stabbing tests with 13.23 J impacting energy. (a), (d), (g) and (j) are the neat Kevlar fabric; (b), (e), (h) and (k) are the composite with 36.23 wt% STF; (c), (f), (i) and (l) are the composite with 103.79 wt% STF.

Open Access Article. Published on 15 August 2017. Downloaded on 15/01/2018 07:53:55.
This article is licensed under a Creative Commons Attribution 3.0 Unported Licence.

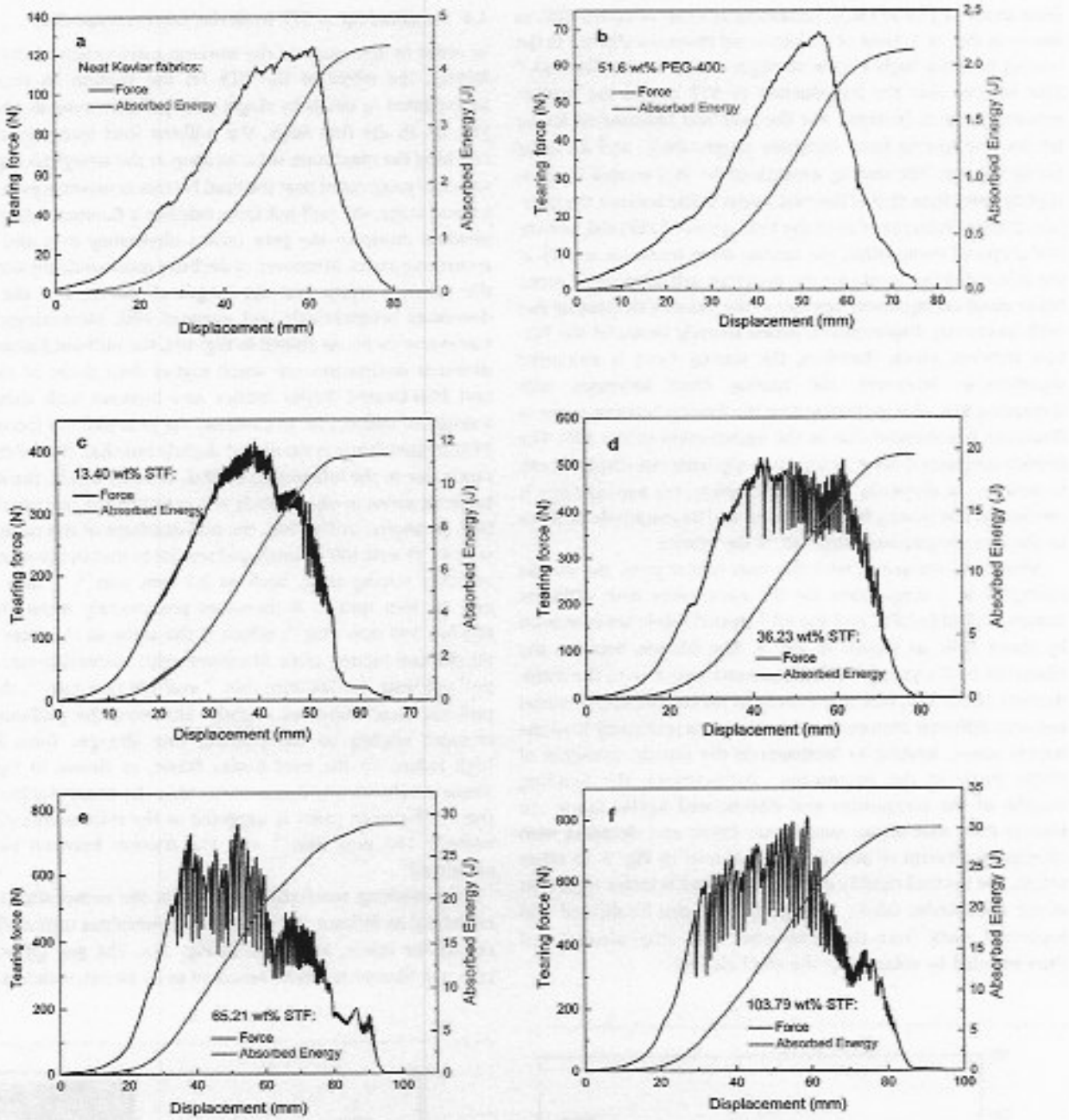


Fig. 7 Tearing strength and energy absorption *vs.* displacement at a rate of 100 mm min^{-1} for (a) the neat Kevlar fabric, (b) the PEG-treated Kevlar fabric, and (c–f) the STF-prepared composites.

the tensile load declined steeply thereafter. However, most of the yarns or filaments slip readily in the neat Kevlar fabric after the loading peak value is obtained (as shown in Fig. S4a in the ESI†); therefore, its elongation at break is higher than that of the composite. It is clear that the tensile strengths of the composites are higher than those of the neat and PEG-treated Kevlar fabrics by 40% to 80%, as shown in Fig. 6b. By increasing the quantity of the added STF, the friction between yarns or filaments may increase; therefore, the tensile strength of the composites is improved. This suggests that the introduction of STF increases the quasi-static tensile strength of the Kevlar fabric.

The results of the quasi-static tearing tests are shown in Fig. 7. It can be clearly seen that the tearing strengths of the neat and PEG-treated Kevlar fabrics are about 120 N and 70 N, respectively, and their absorbed energies are about 4.5 J and 2.1 J, respectively, as shown in Fig. 7a and b. However, both the tearing strength and the absorbed energy increase significantly for the STF-prepared composites; the tearing strength increases from about 400 N to 800 N and the absorbed energy increases

Open Access Article. Published on 15 August 2017. Downloaded on 15/01/2018 07:53:55.
This article is licensed under a Creative Commons Attribution 3.0 Unported Licence.

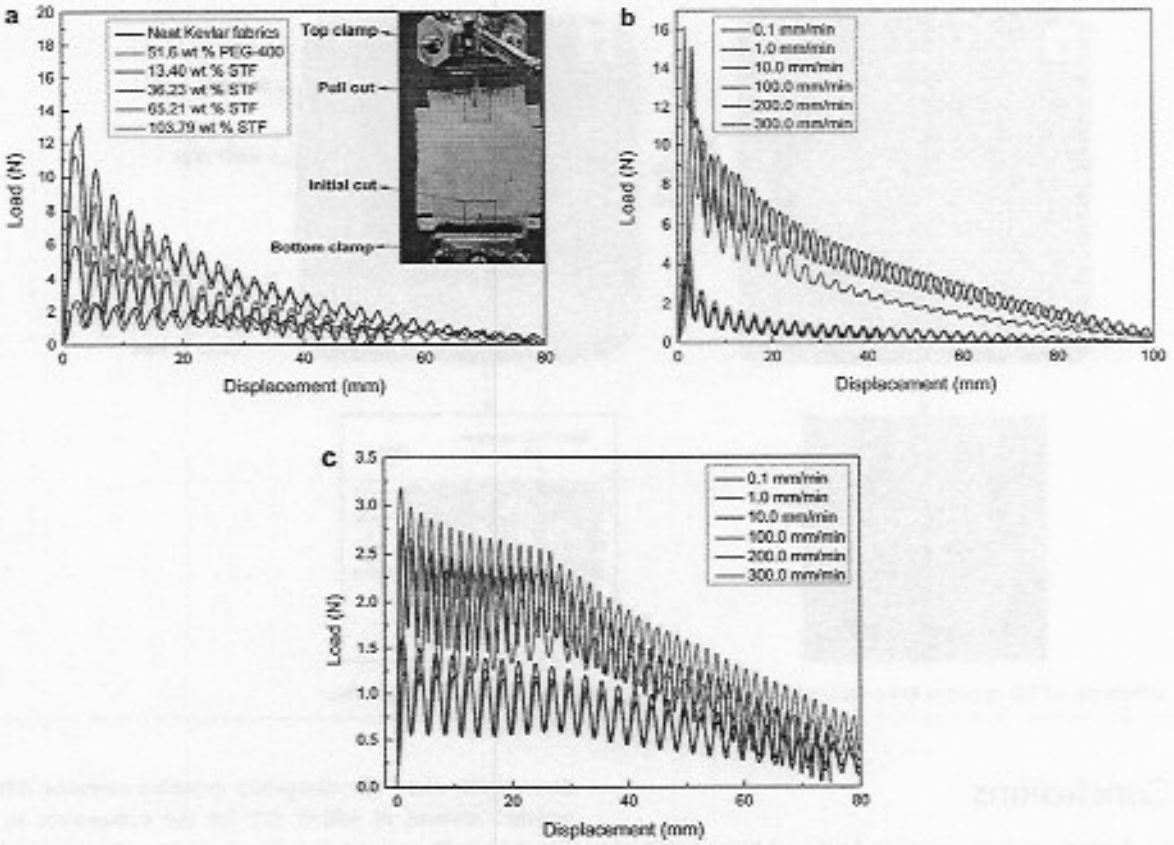


Fig. 10 Tensile load vs. displacement for (a) Kevlar fabrics treated by different methods at a constant rate of 100 mm min^{-1} and (b) the STF-prepared fabric composite with 65.21 wt% STF and (c) the neat Kevlar fabric at different rates.

than the practical value, as shown in Fig. 4k and l. The critical shear rate (γ) is about 4 s^{-1} for the 70 wt% STF, as shown in Fig. 2. The minimum critical velocity (v), estimated by the equation $\frac{dv}{dy} = \gamma$, is only about 2.4 mm min^{-1}. In other words, the shear thickening behavior can be triggered easily as soon as the yarns or filaments experience a relative motion under the knife impact, as shown in the inset of Fig. 11b. The distributed STF in the fabric acts as a bridging or matrix phase due to the very high viscosity of STF, and some silica microspheres may be jammed in the gaps between filaments, as shown in the inset of Fig. 11b. This causes stress to transfer between yarns or filaments, and more yarns or filaments function as an element to sustain the external dynamic or quasi-static impact, as shown in Fig. 11b. Thus, more energy can be absorbed and the composites can endure much higher forces during dynamic or quasi-static knife impact. In the quasi-static mechanical tests, the testing rate, 100 mm min^{-1}, is much higher than the critical velocity; therefore, the shear thickening behavior of the STF can be triggered easily. This causes a prominent increase in the friction between yarns or filaments in the composites, and both the tensile strength and the tearing strength are enhanced. The tearing forces fluctuate in the composites, and the fluctuated amplitude increases with increasing amount of added STF. One possible reason is that the coupling between yarns or filaments will be destroyed when the external force is sufficiently strong; therefore, the tearing force declines sharply. However, new couplings will form quickly due to the reversible and transient response ability of STF, leading to a sharp increase in the tearing force. Moreover, the enhanced quasi-static mechanical properties, including the tensile strength and tearing strength, may also lead to improvements in the dynamic knife-stabbing resistance.

The dynamic knife-stabbing resistance decreases for composites containing an excessive quantity of STFs. One possible explanation is that the impacting behavior may not be optimized at the maximum friction but at some intermediate, tuned degree of mobility. Therefore, the yarns in the composites may be free to move to a certain extent, absorbing energy, lengthening the interaction time with the knife under impact, and decreasing the severity of the instantaneous stresses on the yarns and filaments. In this scenario, the very high pull-out force of the composites is detrimental to the overall stabbing performance, while enough slippage is permitted to reduce instantaneous stress concentrations in the vicinity of the impact. This example underscores an important conclusion that increased friction between yarns or filaments is not always beneficial. It is more likely that an optimal amount of added STF exists for these composites to resist knife impacts.

Open Access Article. Published on 15 August 2017. Downloaded on 15/01/2018 07:53:55.
This article is licensed under a Creative Commons Attribution 3.0 Unported Licence.

5 M. Liu, W. Q. Jiang, Q. Chen, S. Wang, Y. Mao, X. L. Gong, K. C. Leung, J. Tian, H. J. Wang and S. H. Xuan, *RSC Adv.*, 2016, **6**(35), 29279–29287.
6 R. Hoffman, *Trans. Soc. Rheol.*, 1972, **16**(1), 155–173.
7 R. Hoffman, *J. Colloid Interface Sci.*, 1974, **46**(3), 491–506.
8 G. Bossis and J. F. Brady, *J. Chem. Phys.*, 1989, **91**(3), 1866–1874.
9 W. H. Boersma, J. Laven and H. N. Stein, *J. Colloid Interface Sci.*, 1992, **149**(1), 10–22.
10 N. J. Wagner and J. F. Brady, *Phys. Today*, 2009, **62**(10), 27–32.
11 X. Cheng, J. H. Mccoy, J. N. Israelachvili and I. Cohen, *Science*, 2011, **333**(6047), 1276–1279.
12 C. Heussinger, *Phys. Rev. E: Stat., Nonlinear, Soft Matter Phys.*, 2013, **88**(5), 050201.
13 D. Lootens, H. V. Damme, Y. Hémar and P. Hébraud, *Phys. Rev. Lett.*, 2005, **95**(26), 268302.
14 A. Fall, N. Huang, F. Bertrand, G. Ovarlez and D. Bonn, *Phys. Rev. Lett.*, 2008, **100**(1), 018301.
15 E. Brown and H. M. Jaeger, *Phys. Rev. Lett.*, 2009, **103**(8), 086001.
16 R. Seto, R. Mari, J. F. Morris and M. M. Denn, *Phys. Rev. Lett.*, 2013, **111**(21), 218301.
17 M. Wyart and M. Cates, *Phys. Rev. Lett.*, 2014, **112**(9), 098302.
18 H. Laun, R. Bung and F. Schmidt, *J. Rheol.*, 1991, **35**(6), 999–1034.
19 R. Yadav, M. Naebe, X. Wang and K. Kandasubramanian, *RSC Adv.*, 2016, **6**(116), 115145–115174.
20 Y. S. Lee, E. D. Wetzel and N. J. Wagner, *J. Mater. Sci.*, 2003, **38**(13), 2825–2833.
21 E. D. Wetzel, Y. S. Lee, R. Egres, K. M. Kirkwood, J. E. Kirkwood and N. J. Wagner, *Proceedings of the AIP Conference Proceedings*, IOP Institute of Physics Publishing Ltd, 2004.
22 M. J. Decker, C. J. Halbach, C. H. Nam, N. J. Wagner and E. D. Wetzel, *Compos. Sci. Technol.*, 2007, **67**(3), 565–578.
23 D. P. Kalman, R. L. Merrill, N. J. Wagner and E. D. Wetzel, *ACS Appl. Mater. Interfaces*, 2009, **1**(11), 2602–2612.
24 B. W. Lee, I. J. Kim and C. G. Kim, *J. Compos. Mater.*, 2009, **43**(23), 2679–2698.
25 T. A. Hassan, V. K. Rangari and S. Jeelani, *Mater. Sci. Eng., A*, 2010, **527**(12), 2892–2899.
26 A. Srivastava, A. Majumdar and B. S. Butola, *Mater. Sci. Eng., A*, 2011, **529**, 224–229.
27 A. Majumdar, B. S. Butola and A. Srivastava, *Mater. Des.*, 2013, **51**, 148–153.
28 A. Majumdar, B. S. Butola and A. Srivastava, *Mater. Des.*, 2013, **46**, 191–198.
29 X. Y. Feng, S. K. Li, Y. Wang, Y. C. Wang and J. X. Liu, *Mater. Des.*, 2014, **64**, 456–461.
30 J. B. Qin, G. C. Zhang, Z. L. Ma, J. T. Li, L. S. Zhou and X. T. Shi, *RSC Adv.*, 2016, **6**(85), 81913–81923.
31 W. Li, D. S. Xiong, X. D. Zhao, L. L. Sun and J. Liu, *Mater. Des.*, 2016, **102**, 162–167.
32 S. Gürgen and M. C. Kuşhan, *Composites, Part A*, 2017, **94**, 50–60.
33 T. J. Kang, K. H. Hong and M. R. Yoo, *Fibers Polym.*, 2010, **11**(5), 719–724.
34 D. P. Kalman, J. B. Schein, J. M. Houghton, C. H. N. Laufer, E. D. Wetzel and N. J. Wagner, *Proceedings of SAMPE*, 2007, vol. 52, pp. 35–38.
35 P. D. Dubrovski, *Text. Res. J.*, 2000, **70**(10), 915–919.